Synthesis of $Ce_{0.1}La_{0.9}MnO_3$ Perovskite for Degradation of Endocrine Disrupting Chemicals under Visible Photons

Supplementary Information

Synthesis of $Ce_{0.1}La_{0.9}MnO_3$ (CLMO) via Facile Hydrothermal approach

$$La(NO_3)_3.6H_2O + 3\ NaOH \longrightarrow La(OH)_3 + 6\ H_2O + 3\ Na(NO_3)_3 \quad (1)$$

$$(NH_4)_2Ce(NO_3)_6 + 4\ NaOH \longrightarrow Ce(OH)_4 + 4\ NaNO_3 + 2\ NH_4NO_3 \quad (2)$$

where (A site = La, Ce)

$$Mn(NO_3)_2.4H_2O + x\ NaOH \longrightarrow Mn(OH)_2 + 4\ H_2O + 2\ Na(NO_3)_3 \quad (3)$$

$$2\ La(OH)_3 + (1\text{-}x)\ Ce(OH)_4 + 2\ Mn(OH)_2 \longrightarrow Mn_2O_3@\ (1\text{-}x)Ce_2O_3@\ La_2O_3 \quad (4)$$

$$Mn_2O_3@\ (1\text{-}x)Ce_2O_3@\ La_2O_3 \xrightarrow[6\ h]{800\ ^0C} \mathbf{Ce_{0.1}La_{0.9}MnO_3\ (CLMO)} \quad (5)$$

Reactions (S1)–(S5): The reaction pathway for the construction of $Ce_{0.1}La_{0.9}MnO_3$ (CLMO) by facile hydrothermal approach

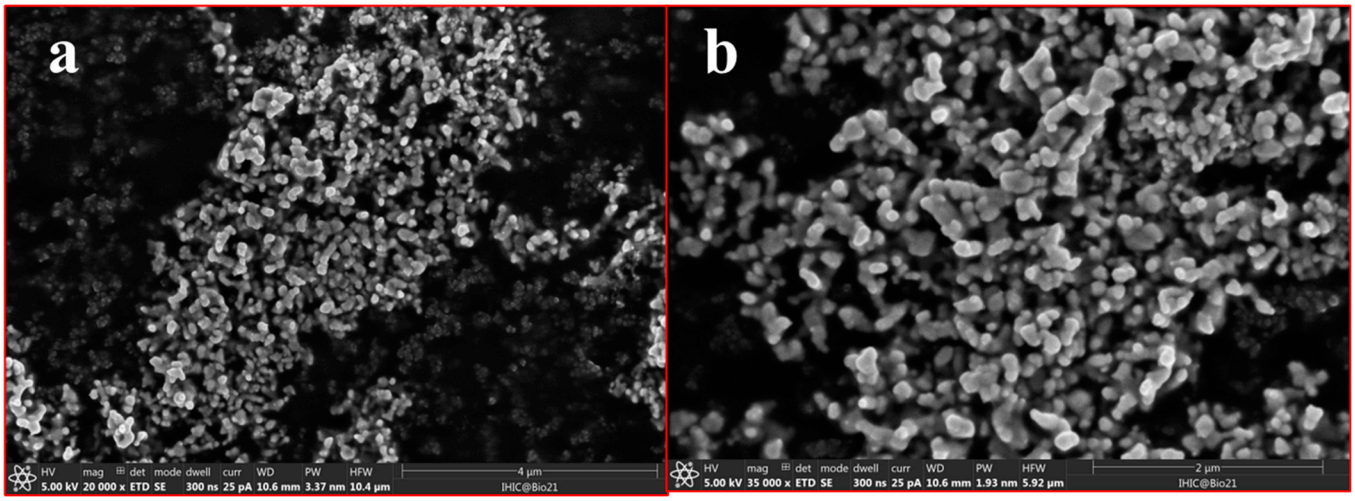

Figure S1: (a-b) FE-SEM image of as-prepared $Ce_{0.1}La_{0.9}MnO_3$ (CLMO) nanostructures.

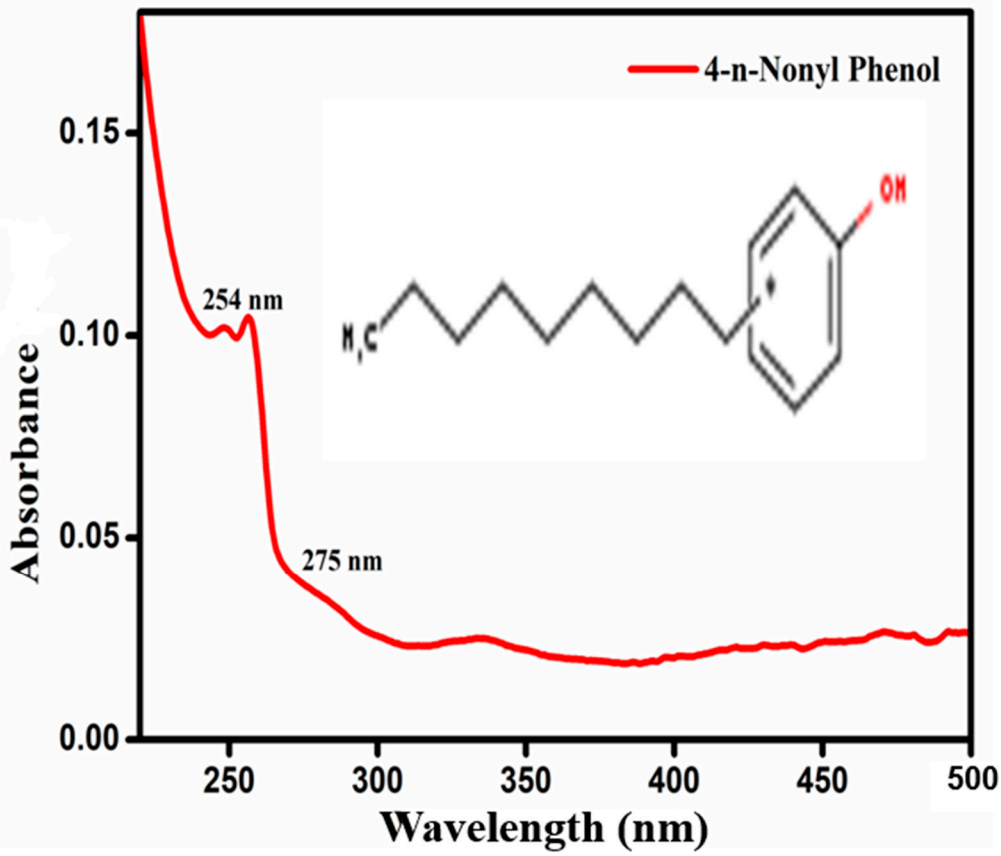

Figure S2: UV-Visible absorption spectrum of 4-*n*-nonylphenol (NP). The inset of the figure provided the molecular structure of NP.

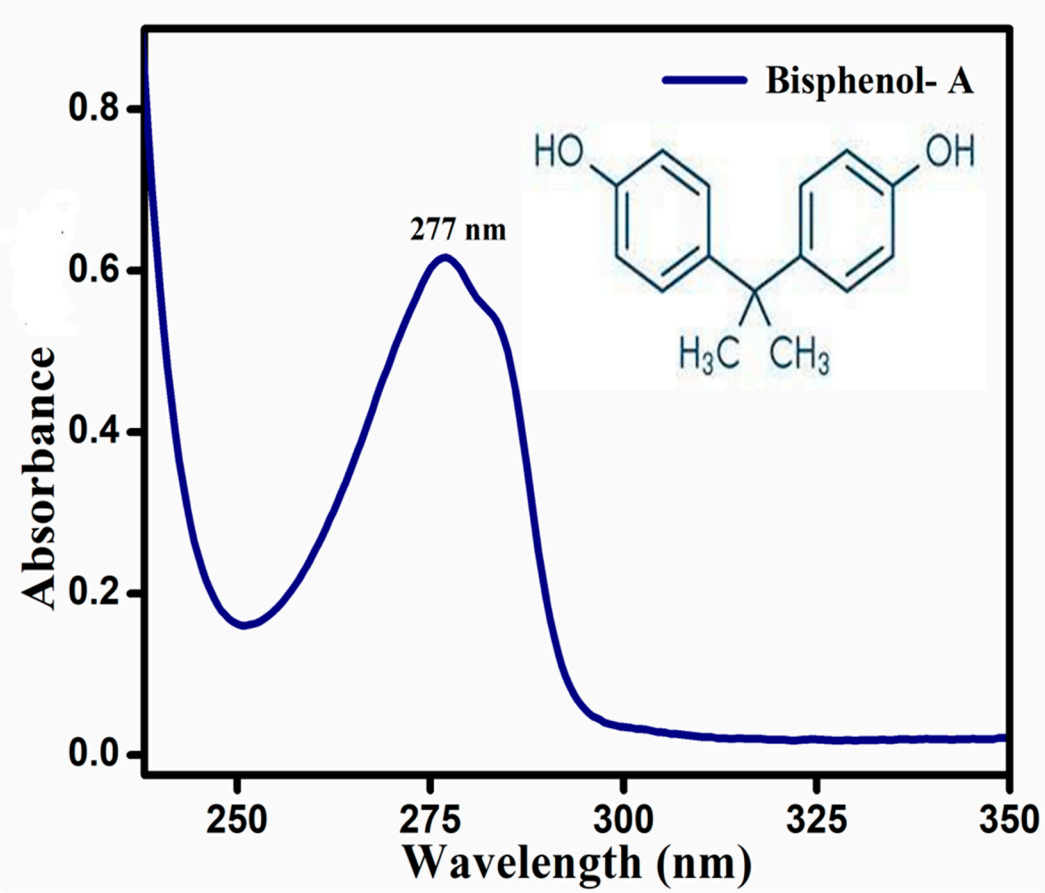

Figure S3: UV-Visible absorption spectrum of Bisphenol-A. The inset of the figure provided the molecular structure of BPA.

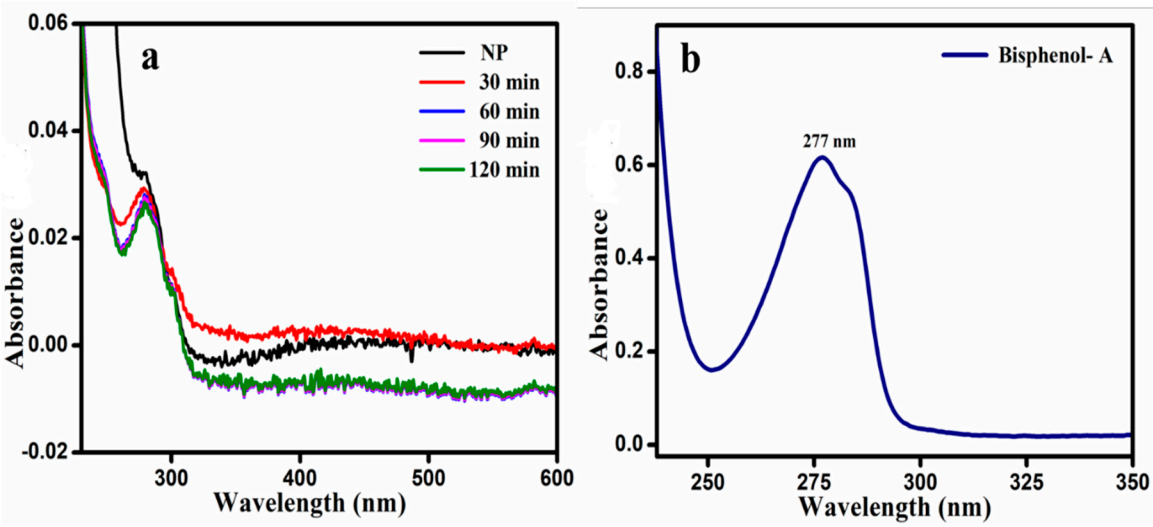

Figure S4: Time dependence UV-Vis absorption spectra of **(a)** NP (4×10^{-4} M) and **(b)** BPA (2×10^{-4} M), respectively, in the absence of catalyst under visible light illumination at pH-7.

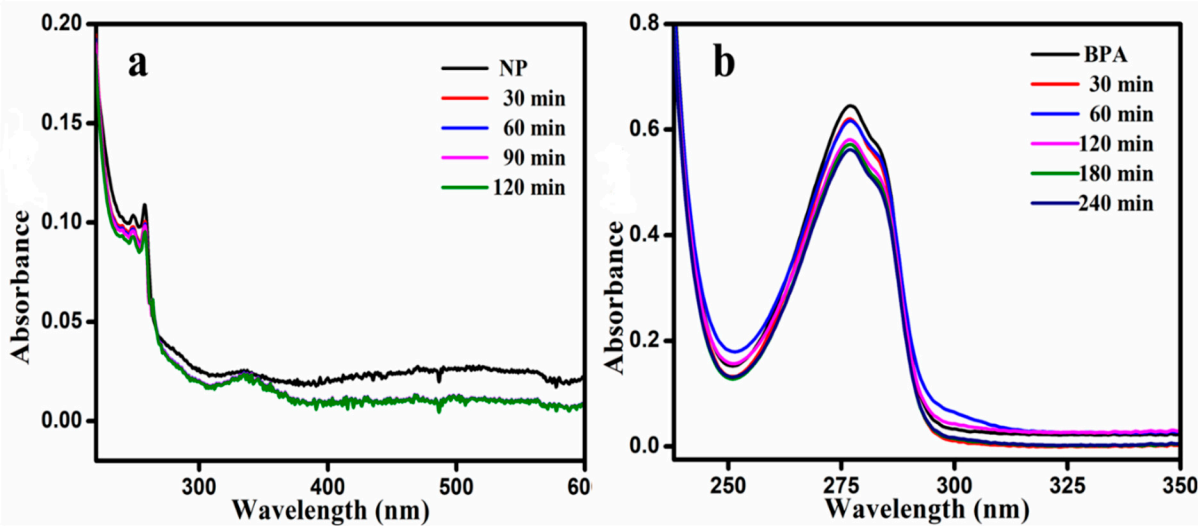

Figure S5: Time dependence UV-Vis absorption spectra of **(a)** NP (4×10^{-4} M) and **(b)** BPA (2×10^{-4} M), respectively, adsorption over CLMO surface; 20 mg/100 mL catalyst dose at pH-7.

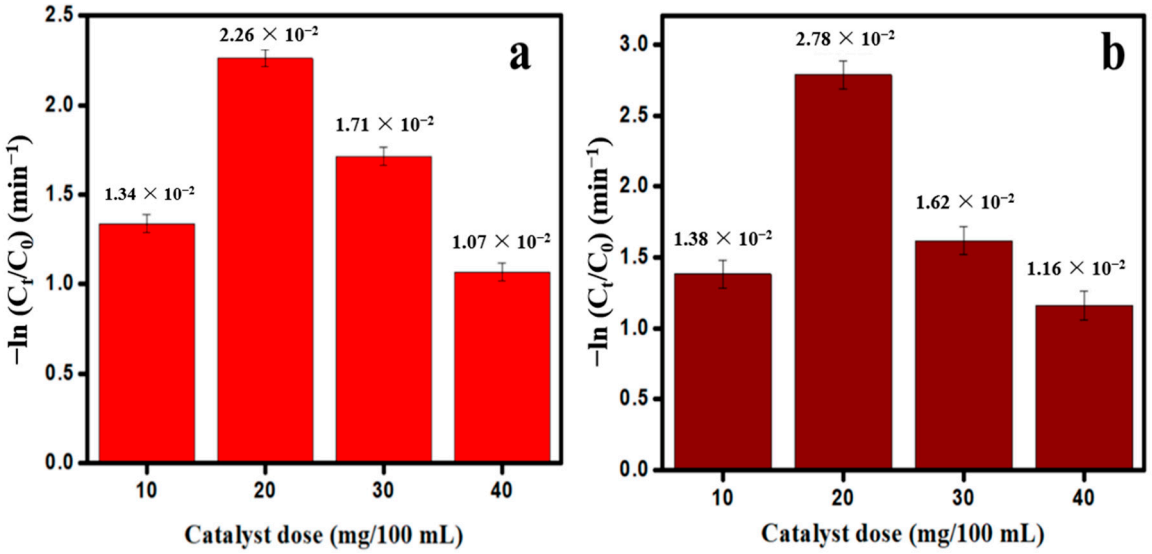

Figure S6: The Pseudo-first-order rate kinetics plots of **(a)** NP and **(b)** BPA pollutants with various quantities of CLMO catalyst loading at pH-7 under the visible photons illumination.

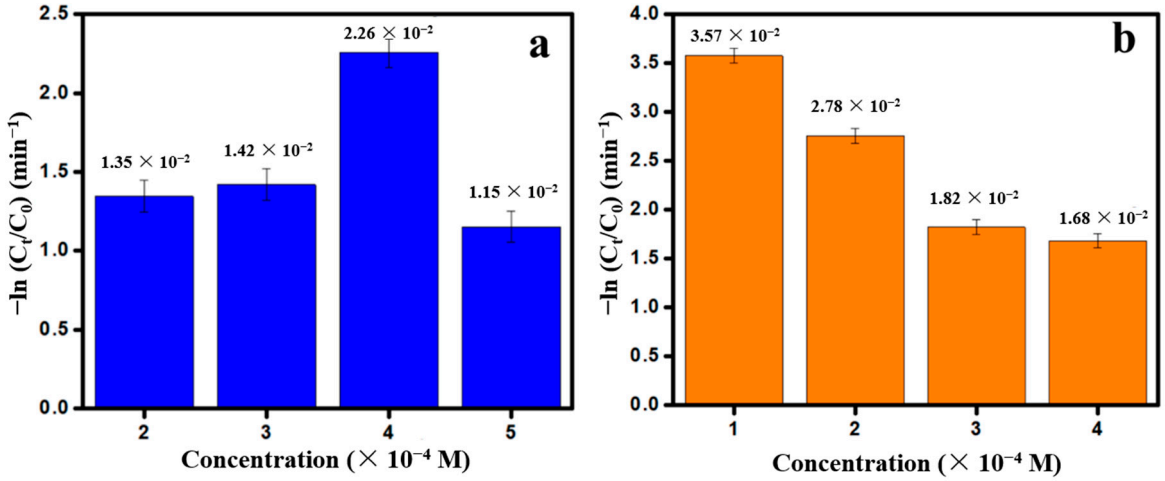

Figure S7: The Pseudo-first-order rate kinetics plots of **(a)** NP and **(b)** BPA pollutants with a different initial concentration of pollutants over CLMO surface at pH-7 under the visible photons illumination.

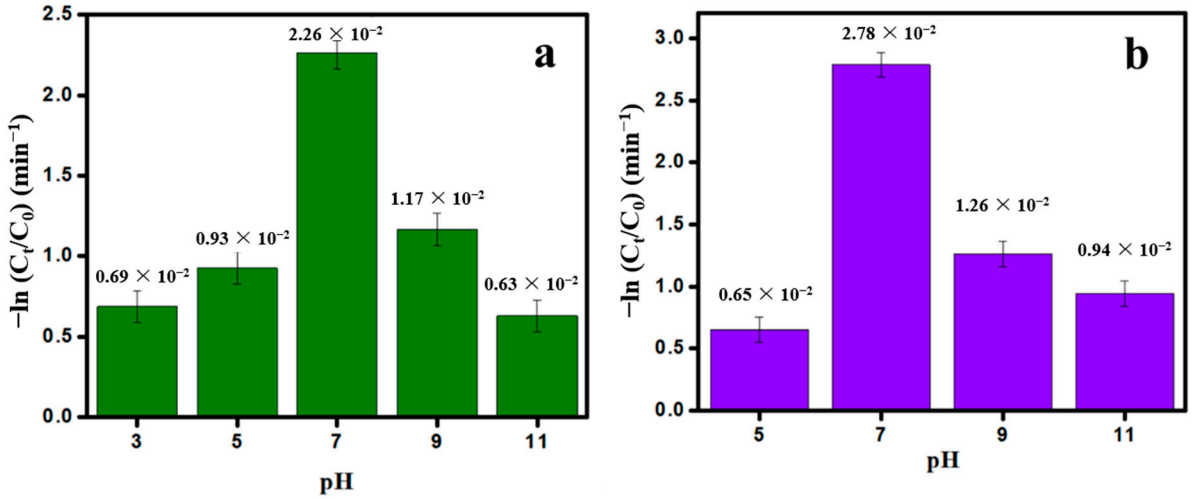

Figure S8: The Pseudo-first-order rate kinetics plots of **(a)** NP and **(b)** BPA pollutants over CLMO surface by varying the pH of the reaction medium under the visible photons illumination.

Table S1: Fourier-transform infrared spectroscopy (FTIR) analysis of NP pollutant before and after photodegradation with CLMO catalyst.

Sl. No	Wave Number (cm^{-1})	Stretching/Bond	Functional Group
	4-n-NonylPhenol (NP) before treatment		
1.	829	C-H ring vibration	
2.	1114	C=C bending	Aromatic ring
3.	1258	C-O stretching	
4.	1614 1515 1466	Aromatic C=C stretching	Aromatic compound
5.	2979 2956 2849	C-H symmetric and asymmetric stretching vibrations	Alkyl chain
6.	3026	C-H aromatic stretching	Aromatic ring
7.	3363	O-H stretching Hydrogen bonded	Phenolic group
	4-n-NonylPhenol (NP) treated over LCMO		
8.	1634	C=C stretching	Cyclic alkene
9.	3347	O-H stretching	Alcohol

Table S2: Fourier-transform infrared spectroscopy (FTIR) measurement of BPA pollutant before and after photodegradation with CLMO catalyst.

Sl. No	Wave Number (cm^{-1})	Stretching/Bond	Functional Group
Bisphenol A (BPA) before treatment			
1.	758	C-C vibration	
2.	828	C-H ring vibrations	
3.	1238	C-O stretching	
4.	1446	C-H scissoring in alkane	Alkyl group
5.	1611 1509	C=C aromatic stretching	Aromatic compound
6.	1881	=C-O stretching	Aromatic Conjugated Alcohol
7.	2964	Aliphatic C-H stretching	Alkyl group
8.	3027	C-H stretching (aromatic)	Aromatic ring
9	3350	O-H stretching Hydrogen bonded	Phenolic group
Bisphenol A (BPA) treated over LCMO			
10.	1636	C=C stretching	Conjugated/Cyclic alkene
11.	3340	O-H stretching	Alcohol

Table S3: Comparison of efficiency and reaction time of Nonylphenol and Bisphenol A using $Ce_{0.1}La_{0.9}MnO_3$ with previously reported TiO_2 based nano catalysts in the literatures.

Catalyst	Pollutants	Catalyst dosage	Irradiation Source	Efficiency and Reaction time	Ref.
Polyvinylidene fluoride (PVDF)/titanium dioxide (TiO_2)	Nonylphenol	1g / 1L	UVA source	85 % in 4 h	1
Carbon-doped TiO_2 (CDT)	Nonylphenol (4 mg/L)	0.2 g/ 0.1 L	Vis source (50W Xenon lamp)	99% within 60 min	2
CuO-TiO_2/GO nanocomposite	Bisphenol A (10 mg/L)	50 mg/ 50 mL	Visible light (5 Philips Mercury (Hg) lamps)	56 % after 300 min	3
Fe-TiO_2/rGO composite	Bisphenol A (95 ppm)	50 mg/ 50 mL	visible light (300-W Xe arc lamp	96 % after 120 min	4
Cyclodextrin polymer (CDP) - TiO_2	Bisphenol A (20 mg/L))	20 mg/ 40 mL	UVA lamps (365 nm, 4 W, F4T5/BLB)	80.2% in 180 min	5
Au–TiO_2	Nonylphenol ethoxylate (NPE)	-----	Sono and Photo source	100 % in 180 min	6
$Ce_{0.1}La_{0.9}MnO_3$	Nonylphenol and Bisphenol A	20mg/ 100 mL	Visible source (Osram halogen lamp)	92 % and 94 % of NP and BPA pollutants are degraded within 120 and 240	Present work

REFERENCE:

1) Hazlini Dzinun, Mohd Hafiz Dzarfan Othman, Ahmad Fauzi Ismail, Mohd Hafiz Puteh, Mukhlis A. Rahman, Juhana Jaafar, *Photocatalytic degradation of nonylphenol by immobilized TiO2 in dual layer hollow fibre membranes*, ***Chemical Engineering Journal,*** 2015, 269, 255–261.
2) Zahra Noorimotlagh, Iraj Kazeminezhad, Neemat Jaafarzadeh, Mehdi Ahmadie, Zahra Ramezanif, *Improved performance of immobilized TiO2 under visible light for the commercial surfactant degradation: Role of carbon doped TiO_2 and anatase/ rutile ratio*, ***Catalysis Today***, 2020, 348, 277–289.
3) Ilknur Altin, *CuO-TiO_2 /graphene ternary nanocomposite for highly efficient visible-light-driven photocatalytic degradation of bisphenol A*, ***Journal of Molecular Structure***, 2022, 1252 ,132199.
4) Huihui Wang, Ning Zhang, Gong Cheng, Han Guo, Zewen Shen, Lu Yang, Yushan Zhao, Ahmed Alsaedi, Tasawar Hayat, Xiangke Wang*, preparing a photocatalytic Fe doped TiO_2/ rGO for enhanced bisphenol A and its analogues degradation in water sample*, ***Applied Surface Science***, 2020, 505, 144640.
5) Esmeralda García-Díaz, Danning Zhang, Yilin Li, Rafael Verduzco, Pedro J.J. Alvarez, *TiO_2 microspheres with cross-linked cyclodextrin coating exhibit improved stability and sustained photocatalytic degradation of bisphenol A in secondary effluent*, ***Water Research***, 2020, 183, 116095.
6) Sambandam Anandan, Muthupandian Ashokkumar, *Sonochemical synthesis of Au–TiO_2 nanoparticles for the sonophotocatalytic degradation of organic pollutants in aqueous environment****, Ultrasonics Sonochemistry***, 2009, 16, 316–320.